Ferroptosis inducer erastin downregulates androgen receptor and its splice variants in castration-resistant prostate cancer

YANRONG YANG[1,2*], TAIYUAN LIU[3*], CHENG HU[4], HONGYAN XIA[4], WEI LIU[5], JUNYU CHEN[6], SHAN WU[6], YU JIANG[1], YANG XU[1], WANXIA LIU[1] and LIJING ZHAO[1]

[1]Department of Recovery, Nursing School, Jilin University, Changchun, Jilin 130021; [2]Department of Cancer Center, School of Medicine, Tongji University, Shanghai 200092; [3]Department of Breast Surgery, The Second Hospital of Dalian Medical University, Dalian, Liaoning 116023; [4]Department of National Engineering Laboratory for AIDS Vaccine, College of Life Sciences, Jilin University; [5]Department of Analysis and Testing Center, Jilin Academy of Environmental Sciences; [6]Department of Gynaecology and Obstetrics, The Second Hospital of Jilin University, Changchun, Jilin 130021, P.R. China

Received August 6, 2020; Accepted December 18, 2020

DOI: 10.3892/or.2021.7976

Abstract. To date, there is no effective therapy available for the treatment of castration-resistant prostate cancer (CRPC), and patients generally succumb to the disease within 2 to 4 years. In the progression of CRPC, androgen receptor (AR) and its splice variants play critical roles. Hence, it is necessary to develop a drug to inhibit the expression and activity of the full-length and splice variants of AR for the treatment of CRPC. Erastin, as the first discovered drug to induce ferroptosis, has been studied in various types of cancer. However, there are few studies focusing on the relationship between erastin and AR. In the present study, western blotting, and sulforhodamine B cell viability, glutathione, lipid peroxidation and reactive oxygen species assays were performed to verify the ferroptosis of CRPC cells; reverse transcription-quantitative polymerase chain reaction, dual-luciferase reporter, and lentiviral packaging and lentivirus-infected cell assays were employed to evaluate how erastin affects AR. A mouse xenograft assay was used to determine the underlying mechanism *in vivo*. Erastin, as a classical inducer of ferroptosis, can suppress the transcriptional activities of both the full-length and splice variants in AR models *in vitro* and *in vivo*. In addition, when erastin was used for CRPC treatment combined with docetaxel, the growth inhibitory efficacy of docetaxel was found to be enhanced. Thus, these findings indicated that ferroptosis inducer erastin has potential in the treatment of CRPC via targeting AR.

Correspondence to: Professor Lijing Zhao, Department of Recovery, Nursing School, Jilin University, 965 Xinjiang Street, Changchun, Jilin 130021, P.R. China
E-mail: zhao_lj@jlu.edu.cn

*Contributed equally

Key words: castration-resistant prostate cancer, erastin, androgen receptor, splice variants

Introduction

In 2018, >1.27 million new cases and 35,800 deaths as a result of prostate cancer were recorded worldwide (1). Prostate cancer accounts for 13.5% of cancers diagnosed in men, which is only lower than lung cancer and is the fifth-leading cause of cancer-related mortality in men. Androgen deprivation therapy (ADT), the main treatment for locally advanced or metastatic androgen-dependent prostate cancer, can alleviate or stabilize symptoms in >80% of patients. However, most patients become non-responsive to this treatment and inevitably progress to castration-resistant prostate cancer (CRPC) following treatment for 12-18 months (2). The serum level of prostate-specific antigen (PSA), one of the most important target genes of androgen receptor (AR) and an important biomarker for the diagnosis and prognosis of prostate cancer, is elevated in patients with CRPC after ADT, suggesting that the AR signaling pathway is reactivated in CRPC cells (3-5). Two major mechanisms are involved in the reactivation of AR in CRPC, including AR upregulation and AR splice variant (AR-V) expression.

AR full-length (AR-FL) is a member of the steroid receptor subfamily that belongs to the nuclear receptor family and consists of four structural domains: Amino-terminal domain, DNA-binding domain, small hinge region and ligand-binding domain (LBD). Activation of the AR signaling pathway mainly depends on androgen, an AR ligand, in prostate cancer cells (5). After binding with its ligand, the AR protein is translocated from the cytoplasm to the nucleus. Two AR molecules are induced to homodimerize by the D-box in the nucleus, and the dimer binds to specific androgen response elements to promote target gene expression (6).

AR-Vs are named based on the majority that lack C-terminal LBD (7) and have constitutive transcriptional activity without

androgen binding (3,8). Several drugs targeting AR reactivation, such as the FDA-approved abiraterone and enzalutamide (MDV3100), can prolong the overall survival of patients with CRPC. However, the majority of patients progress to drug-resistant disease partly because of AR-V expression, which is unaffected by these drugs; therefore, it is necessary to develop novel drugs targeting both AR-FL and AR-Vs to combat CRPC.

Erastin was first discovered to kill cancer cells overexpressing H-ras in engineered tumorigenic cells by synthetic lethal high-throughput screening of >20,000 compounds in 2003 (9). When erastin induces cell death, neither chromatin fragmentation nor caspase activation is detected, and the levels of intracellular reactive oxygen species (ROS) are upregulated and erastin-induced death can be prevented by iron chelation. In 2012, Dixon *et al* (10) proposed the term ferroptosis to describe this new death pattern. Erastin can induce ferroptosis via different mechanisms, such as directly targeting mitochondrial voltage-dependent anion channels (11), inhibiting the activity of the xCT light chain of the cystine/glutamate transporter (also known as system XC-) (12,13), playing a relevant role in the MAPK pathway (14) and increasing heme oxygenase-1 (15,16). Furthermore, Hasegawa *et al* (17) found that mucin 1 C-terminal subunit/xCT can downregulate erastin-induced ferroptosis in triple-negative breast cancer. As an inducer of ferroptosis, erastin has been demonstrated to inhibit cancer cell proliferation in acute myeloid leukemia, and hepatocellular, breast, ovarian, and head and neck cancer (16-18), although the mechanisms attributed to cell death differ among these cancers. Although a considerable number of studies have sought to determine whether erastin inhibits prostate cancer, it is necessary to investigate the specific mechanism of erastin, such as the activation of the AR signaling pathway in prostate cancer cells, specifically in CRPC.

Materials and methods

Prostate cancer cell lines and reagents. LNCaP, PC3, 22Rv1, C4-2, C4-2B, Du145 and 293T cells were obtained from the American Type Culture Collection. These cells were cultured in RPMI-1640 (Gibco; Thermo Fisher Scientific, Inc.) medium supplemented with 10% fetal bovine serum (FBS; Clark Bioscience) at 37˚C in a humidified atmosphere with 5% CO_2. LNCaP95 cells were provided by Dr Alan Meeker at the Johns Hopkins University (Baltimore, MD, USA) and were cultured in RPMI-1640 medium supplemented with 10% charcoal-stripped FBS (Gibco; Thermo Fisher Scientific, Inc.). Erastin, docetaxel (DTX), ferrostatin-1, liproxstatin-1, ZVAD-FMK, necrosulfonamide and chloroquine were purchased from Selleck Chemicals.

Sulforhodamine B (SRB) cell viability assay. After being treated with erastin at different concentrations (0, 2.5, 5.0, 10.0, 20.0 or 40.0 μM) for 24, 48 or 72 h, cell monolayers of 22Rv1 or LNCaP95 in 96-well plates were fixed using 20% (wt/vol) trichloroacetic acid (100 μl/well) at room temperature for at least 3 h, and then stained for 30 min using SRB (Shanghai YuanYe Biotechnology Co., Ltd.) at room temperature. Excess dye was removed by washing repeatedly with 1% (vol/vol) acetic acid. The protein-bound dye was dissolved in 10 mM Tris base solution and then the OD was measured at 565 nm using a Multiscan Spectrum spectrophotometer. In order to obtain more samples in the subsequent experiments, the doses of erastin were determined based on the cell inhibition rate of 30%. Thus, 22Rv1 and LNCaP95 cells were treated with 10 or 20 μM erastin, while PC3 cells were treated with 1 μM erastin.

In order to verify whether the effect caused by erastin was ferroptosis, the cells were treated with erastin (20 μM). Meanwhile, the cells were added with or without ferroptosis inhibitors (1 μM ferrostatin-1 or 1 μM liproxstatin-1), apoptosis inhibitor (10 μM ZVAD-FMK), necroptosis inhibitor (1 μM necrosulfonamide), or autophagy inhibitor (25 μM chloroquine). After treatment for 48 h, the cell viability was detected by SRB as described above.

In order to calculate the combination index (CI) between DTX and erastin, 22Rv1 and LNCaP95 cells were treated with these two drugs at different concentrations (0, 2.5, 5.0 or 10.0 μM erastin and 0, 5, 10 nM DTX). After treatment for 48 h, cell viability was detected by SRB as described above.

Western blot analysis. Western blotting was conducted as previously described (19), and proteins were visualized using an Odyssey Infrared Imaging System (LI-COR Biosciences), following the manufacturer's protocols. Glyceraldehyde-3-phosphate dehydrogenase (GAPDH) was used for normalization of the densitometry signals. The following antibodies were used in this study: Anti-N-terminal AR antibody (cat. no. 5153; 1:1,000; Cell Signaling Technology, Inc.), anti-phospholipid hydroperoxide glutathione peroxidase (GPX4; cat. no. ab125066; 1:1,000; Abcam) and anti-GAPDH (cat. no. A00227; 1:1,000; Wuhan Boster Biological Technology, Ltd.). IRDye® 800CW goat anti-human IgG (H+L) (cat. no. 926-32232; 1:10,000; LI-COR Biosciences).

ROS assay. After treatment with erastin for 24 h, the cells were incubated with 1 μl DCFH-DA with 1 ml phosphate-buffered saline (PBS) for 1 h at 37˚C in the dark to assess the cytosolic ROS levels. Samples were centrifuged at 860 x g at room temperature for 3 min, and the pellets were resuspended in 1 ml PBS. Measurements were performed on a FACSCalibur™ (BD Biosciences) flow cytometer using FlowJo software 7.6 (FlowJo LLC). All experimental results are reported as represented by three replicates.

Glutathione (GSH) and lipid peroxidation assays. The GSH and malondialdehyde (MDA) contents in cell lysates were assessed using GSH (cat. no. A061-1-2) and lipid peroxidation (cat. no. A003-4-1) assay kits, respectively, according to the manufacturer's instructions. Both kits were purchased from Nanjing Jiancheng Bioengineering Institute.

Dual-luciferase reporter gene assay. Three luciferase reporter plasmids were used in this research, and transfection was performed with TurboFect Transfection Reagent (cat. no. R0531; Thermo Fisher Scientific, Inc.). The androgen-responsive element-luciferase plasmid contains three repeat ARE regions ligated in tandem to a

luciferase reporter (ARR3-Luc), which was provided by Dr Robert Matusik at Vanderbilt University School of Medicine (Nashville, TN, USA), and was used to reflect the AR-FL trans-activation activity. The ubiquitin-conjugating enzyme E2C-luciferase plasmid (UBE2C-luc) is driven by a minimal promoter and three repeats of an AR-V-specific promoter element. Thus, it was used to reflect AR-V7 trans-activation activity. pGL4-ARpro8.0 is driven by an 8.0 kb fragment of the 5'-flanking region of the human AR gene. The transfected cells, including 22Rv1, LNCaP95, PC3 and LNCaP cells, were divided equally into 24-well plates ($1x10^5$ cells/well) and cultivated in serum-free medium for 24 h. Subsequently, the cells were exposed to charcoal-stripped FBS with or without 1 nM R1881 (Sigma-Aldrich; Merck KGaA) at 37˚C, which is a type of synthetic androgen, and erastin to detect AR-FL or AR-V7 activity. After 24 h, the cells were lysed with 100 μl reporter lysis buffer (Promega Corporation), and the luciferase activity was assayed using the Luciferase Assay System (Promega Corporation) and normalized based on the protein concentrations for each sample.

Reverse transcription-quantitative polymerase chain reaction (RT-qPCR). The total RNA of cells was extracted and collected using an E.Z.N.A.® Total RNA Kit I (Omega Bio-Tek, Inc.) and quantified with a NanoDrop™ spectrophotometer (Thermo Fisher Scientific, Inc.). Reverse transcription was performed with an RNA reverse transcription kit (Takara Bio, Inc.), and qPCR was performed using TransStart® Green qPCR SuperMix (TransGen Biotech Co., Ltd.), according to the manufacturer's instructions for 45 cycles of 5 sec at 94˚C and 30 sec at 60˚C. 36B4 served as the normalization control for these qPCR assays. The following primers were used: AR-FL sense, 5'-GTACAGCCAGTGTGTCCGAA-3' and anti-sense, 5'-TTGGTGAGCTGGTAGAAGCG-3'; AR-V7 sense, 5'-AAAAGAGCCGCTGAAGGGAA-3' and anti-sense, 5'-GCCAACCCGGAATTTTTCTCC-3'; PSA sense, 5'-CTCAGGCCAGGTGATGACTC-3' and anti-sense, 5'-GTCCAGCACACAGCATGAAC-3'; transmembrane protease serine 2 (TMPRSS2) sense, 5'-ACACACCGATTCTCGTCCT-3' and anti-sense, 5'-TGGCCTACTCTGGAAGTTCA-3'; UBE2C sense, 5'-TTCCCCAGTGGCTACCCTTA-3' and anti-sense, 5'-CAGGGCAGACCACTTTTCCT-3'; transcription factor E2F7 (E2F7) sense, 5'-TTCTGTTGCTCAGACGGACC-3' and anti-sense, 5'-ATCCCTCTCTGACCCTGACC-3'; and 36B4 sense, 5'-CGACCTGGAAGTCCAACTAC-3' and anti-sense, 5'-ATCTGCTGCATCTGCTTG-3'. mRNA expression levels were quantified using the $2^{-\Delta\Delta Cq}$ method (20).

Lentiviral packaging and lentivirus-infected cells. Three plasmids were used as lentiviral vectors: VSVG, Δ8.2, pLVX-AR-FL or pLVX-AR-V7. VSVG, Δ8.2, and oLVX were provided by the National Engineering Laboratory for AIDS Vaccine (Jilin University, Changchun, China). The preparation of the lentiviral particles and lentiviral infections were performed as previously described (21). When lentiviral particles (collected at 48 h after transfection) were used to infect 22Rv1 cells in 6-well plates ($1x10^6$ cells/well), polybrene was added at a final concentration of 6 μg/ml, fresh medium was replaced within 6 h, and the protein expression was determined by western blotting.

22Rv1 tumor xenograft model. A total number of 12 male BALB/c nude mice (age, 6-8 weeks old; weight, 15-20 g) were purchased from Beijing Vital River Laboratory Animal Technology Co., Ltd. All mice were housed at a constant temperature and constant humidity in a specific pathogen-free environment with free access to food and water. The present study was approved by the Animal Ethics Committee of Basic Medical College of Jilin University (approval no. 2016045). After 1 week of adaptation, $5x10^6$ 22Rv1 cells suspended in 50% Matrigel and PBS were injected subcutaneously into the right dorsal flank. Tumor formation was strictly monitored, and tumor volume was calculated by the modified ellipsoidal formula: Tumor volume = 0.52 x length x $width^2$. When the tumor size reached ~50 mm^3, the mice were randomly allocated into two groups (n=6/per group) and treated with or without erastin. The dose of erastin administered to the mice was 20 mg/kg, which was injected intraperitoneally twice every other day. After being treated for 2 weeks, all mice were injected with pentobarbital sodium at a dose of 20 mg/kg intraperitoneally. Then, 0.5 ml mouse blood was collected from the orbital vein to detect serum prostate-specific antigen (PSA) levels using a human KLK3 ELISA Kit (cat. no. KIT10771; Sino Biological, Inc.), tumors were removed for molecular analysis, and some organs were removed for a safety evaluation at the end of the experiment. Finally, all mice were sacrificed by intraperitoneal injection with pentobarbital sodium at a dose of 150 mg/kg. Erastin was dissolved in 3.3% dimethyl sulfoxide (DMSO) and 96.7% β-cyclodextrin (20%).

Histopathology assay. Hematoxylin and eosin (H&E) staining was performed as described in a previous study (22). Briefly, the tissues of the rats were fixed in 10% buffered formalin, and then decalcified in 10% ethylenediaminetetraacetic acid. The tissues were then treated with ethanol and xylene for dehydration. After being embedded in paraffin and sliced, several 4-μm thick histological slices were stained with H&E. The images were subsequently acquired using a light microscope (BX51; Olympus Corporation) at x200 magnification.

Immunohistochemistry (IHC). IHC staining was performed as described previously (23). Briefly, histological slices from tumor tissues were stained with anti-N-terminal AR antibody (1:200; cat. no. 5153; Cell Signaling Technology, Inc.). Histological images were captured by a microscope (BX51; Olympus Corporation) with an objective magnification of x200.

Statistical analysis. The experiments were repeated three times independently. Statistical analysis was performed for multiple comparisons using one factor analysis of variance (ANOVA) followed by Dunnett's or Bonferroni's post hoc tests. All data were analyzed with the statistical software SPSS 11.0 (SPSS, Inc.), and the results are expressed as the mean ± SD. $P<0.05$ was considered to indicate a statistically significant difference. SPSS software was also used to calculate the CI, a CI value of >1, 1 and <1 denotes antagonism, additivity and synergism, respectively.

Results

Erastin inhibits the growth of CRPC cells. Western blotting was employed to detect the expression of AR, AR-Vs and

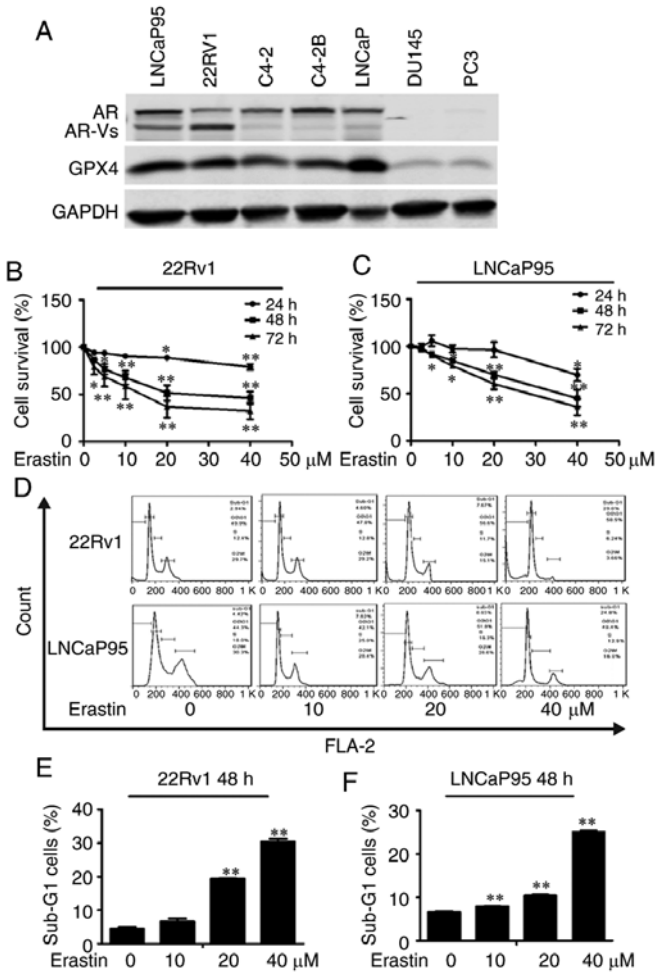

Figure 1. Erastin inhibits the proliferation of castration-resistant prostate cancer cells. (A) The protein expression of AR, AR-Vs and GPX4 in prostate cancer cell lines. (B and C) Sulforhodamine B assays showed that erastin inhibited the proliferation of 22Rv1 and LNCaP95 cells in a dose-dependent manner. (D-F) The proportion of sub-G1 cells was increased in 22Rv1 and LNCaP95 cells after treatment with erastin for 48 h. Statistical analysis was performed using ANOVA followed by Dunnett's post hoc test. $^{*}P<0.05$ and $^{**}P<0.01$ vs. control. AR, androgen receptor; AR-V, AR splice variant; GPX4, phospholipid hydroperoxide glutathione peroxidase.

GPX4 in several prostate cancer cell lines including LNCaP95, LNCaP, Du145, C4-2B, 22Rv1, C4-2 and PC3 cells. The results showed that both 22Rv1 and LNCaP95 cell lines expressed AR, AR-Vs and GPX4 (Fig. 1A). Conversely, PC3 cells did not express AR or AR-Vs and only showed a low expression of GPX4. Thus, 22Rv1, LNCaP95 and PC3 cell lines were chosen for the subsequent experiments.

The effect of erastin on the proliferation of 22Rv1 and LNCaP95 cells was detected by the SRB assay. As presented in Fig. 1B and C, erastin inhibited the proliferation of these two CRPC cell lines in a dose-dependent manner. Then, PI flow cytometry was employed to examine the effect of erastin on the cell cycle. The results showed that erastin could increase the proportion of cells in sub-G1 phase and cause cycle arrest (Fig. 1D-F).

Erastin induces ferroptosis in CRPC cells. To verify that the effect caused by erastin is ferroptosis, the cells were treated with erastin with or without ferroptosis inhibitors (ferrostatin-1 and liproxstatin-1), apoptosis inhibitor (ZVAD-FMK), necroptosis inhibitor (necrosulfonamide) and autophagy inhibitor (chloroquine). The SRB results showed that in both cell lines, ZVAD-FMK, necrosulfonamide and chloroquine had no effect on erastin-induced cell death (Fig. 2A and B). The death of the 22Rv1 cells induced by erastin was only reversed by ferrostatin-1 and liproxstatin-1.

Then, the expression of the ferroptosis marker protein GPX4 was measured. The results showed that erastin downregulated the protein expression of GPX4 in both cell lines (Fig. 2C and D). Given that ferroptosis is characterized by lipid peroxidation, the level of GSH, a key regulator that maintains cellular redox homeostasis, was investigated. The results showed that ROS levels in both cell lines were increased with erastin treatment compared with the control group (Fig. 2E and F). Moreover, GSH levels were downregulated after erastin treatment in these two cell lines (Fig. 2G and H). MDA, an end product of lipid peroxidation, was notably increased following erastin treatment, as expected (Fig. 2I and J). According to the aforementioned results, it was hypothesized that ferroptosis was initiated in these two cell lines after erastin treatment.

Erastin downregulates AR protein expression by inhibiting the transcription of the AR gene. Given that AR-FL and AR-Vs play important roles in the development of CRPC, 22Rv1 and LNCaP95 CRPC cells that express AR-FL and AR-Vs were chosen in the present study to explore whether erastin can inhibit AR expression. In 22Rv1 cells, AR-Vs include AR-V7 (also called AR3), AR-V1 (also called AR4) and AR-V4 (also called AR5) (8,24), whereas LNCaP95 cells express only AR-V7 (25). Among these splice variants, AR-V7 has been found to be associated with the development of CRPC and is recognized as a biomarker of poor prognosis for patients with CRPC (26); thus, AR-V7 was selected as the representative of AR-Vs in the present study. The expression of AR-FL and AR-V proteins was detected by western blotting, and the results showed that erastin downregulated both AR-FL and AR-V protein expression levels (Fig. 3A and B).

To investigate how erastin decreases the protein levels of AR-FL and AR-V, AR-FL and AR-V7 mRNA expression levels were measured by RT-qPCR. As expected, erastin significantly reduced the levels of AR-FL and AR-V7 mRNA (Fig. 3C and D). Then, AR promoter activity was detected using dual-luciferase reporter plasmid pGL4-ARpro8.0. Erastin treatment resulted in the significant inhibition of AR promoter activity in both cell lines (Fig. 3E and F). Taken together, the data indicated that erastin had the ability to inhibit the transcription of the AR gene in CRPC cells.

Erastin downregulates AR-FL and AR-V transactivation. To evaluate the effects of erastin on AR transactivation, AR-FL and AR-V transcriptional activity and their target genes were measured by a reporter gene assay and RT-qPCR, respectively. First, 22Rv1 cells were transfected with the ARR3-luc luciferase construct, which contained three tandem repeats of androgen response elements. The results showed that erastin treatment induced a reduction in luciferase activity in 22Rv1 cells (Fig. 4A). Considering that the ARR3-luc construct can be regulated not only by AR-FL, but also by AR-Vs, the

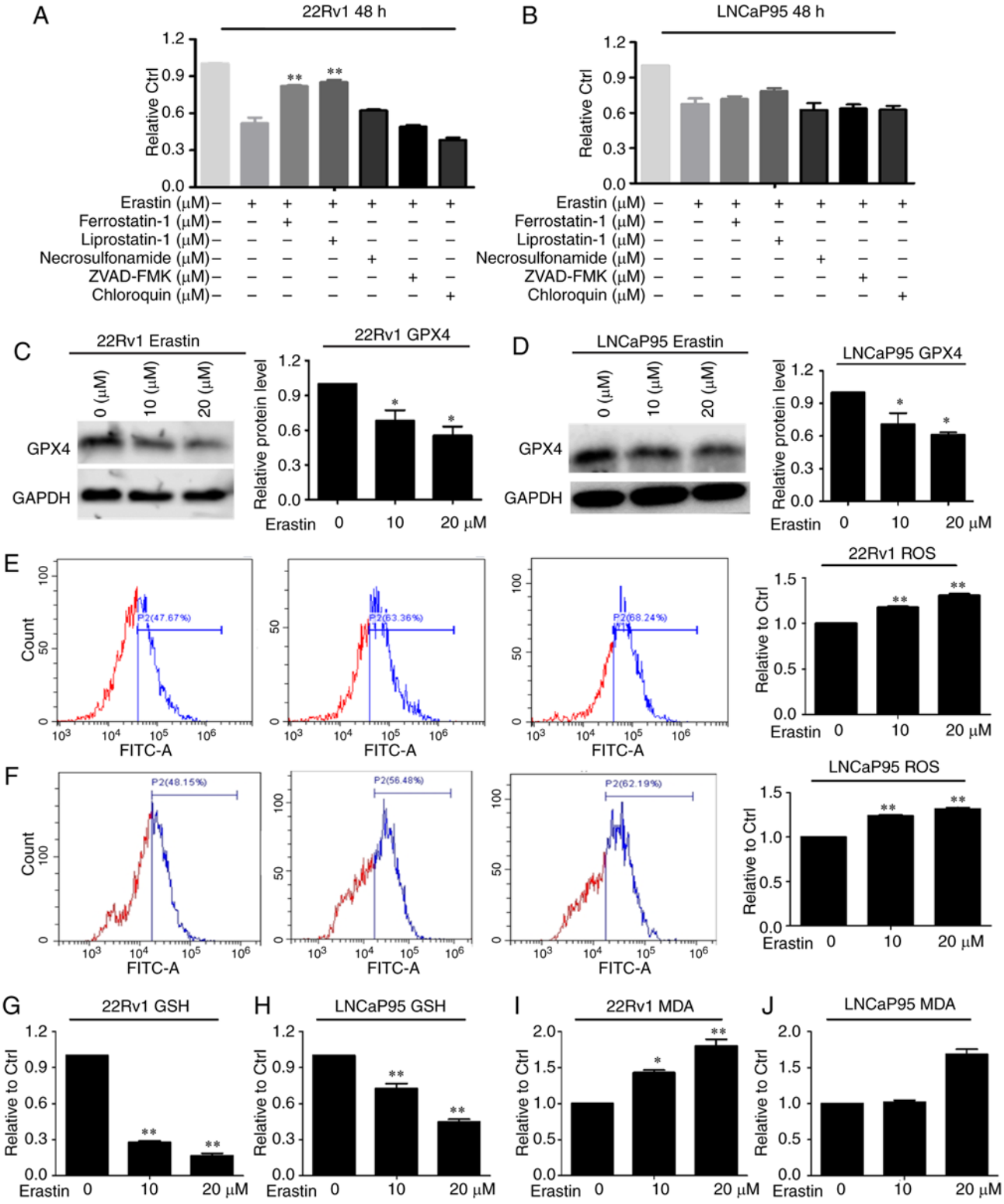

Figure 2. Erastin induces ferroptosis in castration-resistant prostate cancer cells. (A and B) 22Rv1 and LNCaP95 cells were treated with 20 μM erastin with or without cell death inhibitor (1 μM ferrostatin-1, 1 μM liproxstatin-1, 10 μM ZVAD-FMK, 1 μM necrosulfonamide or 25 μM chloroquine) for 48 h. (C and D) The expression of GPX4 protein in 22Rv1 and LNCaP95 cells after treatment with erastin for 48 h. (E and F) ROS levels were assayed in the 22Rv1 and LNCaP95 cells treated with 10 or 20 μM erastin for 24 h. (G and H) GSH levels were assayed in the 22Rv1 and LNCaP95 cells treated with 10 or 20 μM erastin for 48 h. (I and J) MDA levels were assayed in the 22Rv1 and LNCaP95 cells treated with 10 and 20 μM erastin for 48 h. Statistical analysis was performed using ANOVA followed by Dunnett's post hoc test. *P<0.05 and **P<0.01 vs. control. GPX4, phospholipid hydroperoxide glutathione peroxidase; ROS, reactive oxygen species; GSH, glutathione; MDA, malondialdehyde.

LNCaP cell line was selected for transfection with a ARR3-luc luciferase construct because these cells only express AR-FL. The results in LNCaP cells clearly showed that erastin inhibited AR-FL trans-activating activity (Fig. 4B). To specifically assess the effect of erastin on AR-V transcriptional activity, 22Rv1 and LNCaP95 cells were transfected with the UBE2C-luc construct

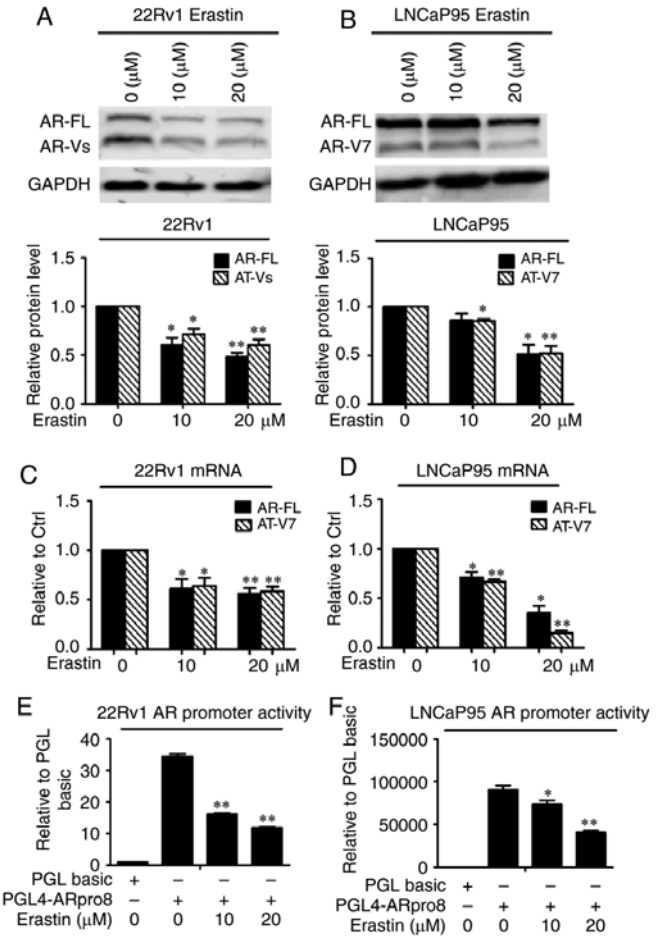

Figure 3. Erastin downregulates AR protein expression by inhibiting the transcription of the AR gene. Erastin downregulated AR-FL and AR-V protein levels in (A) 22Rv1 and (B) LNCaP95 cells treated with 10 and 20 μM erastin for 48 h. Reverse transcription-quantitative PCR analysis showed that erastin at 10 and 20 μM decreased AR-FL and AR-V mRNA levels in (C) 22Rv1 and (D) LNCaP95 cells. Luciferase assays showed that erastin inhibited the activity of the 8.0 kb proximal AR promoter in (E) 22Rv1 and (F) LNCaP95 cells. Cells transfected with the pGL4-ARpro8.0 construct were treated with 10 or 20 μM erastin for 24 h. Statistical analysis was performed using ANOVA followed by Dunnett's post hoc test. *P<0.05 and **P<0.01 vs. control. AR, androgen receptor; AR-V, AR splice variant; AR-FL, AR full-length.

in which the luciferase gene is driven by an AR-V-specific promoter element of the UBE2C gene (27). Most of the AR-Vs identified to date display constitutive activity, when AR-V transcriptional activity was measured (28); therefore, these cells were cultured with 10% charcoal-stripped FBS. As shown in Fig. 4C and D, erastin caused the effective inhibition of AR-V trans-activating activity.

Considering that erastin had a significant inhibitory effect on endogenous AR-FL and AR-V transcriptional activity, it was speculated that erastin had an inhibitory effect on exogenous AR activity. To test this hypothesis, the effect of erastin on exogenously expressed AR-FL and AR-V7 trans-activating activity was evaluated in the PC-3 cell line (null-AR). The results showed that PC3 cells were significantly inhibited and the exogenous AR-FL and AR-V trans-activating activity was evidently decreased after the treatment of 1 μM erastin (Fig. 4E-G). The exogenous AR-V7 trans-activating activity was further tested in LNCaP cells (without AR-Vs), and the results were consistent with those of the PC3 cells (Fig. 4H).

Consistently, the mRNA levels of the AR-FL target genes PSA and TMPRSS2 and the AR-V-specific target genes UBE2C and E2F7 were significantly downregulated by erastin in both the 22Rv1 and LNCaP95 cell lines (Fig. 4I-L). Collectively, these findings indicated that erastin could downregulate AR-FL and AR-V trans-activation.

Upregulation of AR-FL and AR-V7 expression reverses the growth inhibition of erastin in 22Rv1 cells. To further test the importance of the roles of AR-FL and AR-V in the action of erastin in CRPC cells, AR-FL and AR-V7 were overexpressed in the 22Rv1 cell line using lentiviral infections that delivered AR-FL and AR-V7 RNA expression constructs, and growth inhibition was evaluated using the SRB method. As shown in Fig. 5A and B, the expression of AR-FL and AR-V7 proteins in the 22Rv1 cells was significantly upregulated, especially the AR-FL protein. The overexpression of AR-FL and AR-V7 significantly promoted the resistance to high concentrations of erastin after 48 and 72 h compared with controls in the 22Rv1 cells. However, there was no significant difference between the overexpression of AR-FL and AR-V7 protein (Fig. 5C and D).

Erastin inhibits the 22Rv1 xenograft tumor growth rate. To investigate whether erastin inhibits the tumor growth *in vivo*, 22Rv1 cells were implanted into the subcutaneous space of immune-deficient nude mice. The tumor growth curve results are shown in Fig. 6A and revealed that erastin inhibited the growth of 22Rv1 tumors, with significance differences found on day 7 of the treatment. At the end of the experiments, the average tumor weight in the control group was 0.80±0.11 g, while that in the erastin-treated group was 0.55±0.17 g (Fig. 6B-D). The results of H&E staining of the tumor tissues showed that the nuclear/cytoplasmic ratio of tumor cells was notably decreased in the erastin group (Fig. 6E). Given that serum PSA concentration is one of most important clinical indexes for the diagnosis of prostate cancer, serum PSA levels were measured by ELISA, and a significant reduction in PSA serum levels in response to erastin treatment was observed (Fig. 6F). Then, AR protein levels were measured using IHC in tumor tissues. In erastin-treated tumor specimens, AR was obviously downregulated (Fig. 6G). In addition, the protein and mRNA levels of AR-FL and AR-V in the tumor tissues were measured by western blotting and RT-qPCR. Both the protein levels and mRNA levels of AR-FL and AR-V7 in the tumor tissues were decreased (Fig. 6H and I), which was consistent with the results obtained *in vitro*.

Evaluation of erastin safety in mice. To evaluate the toxicity of erastin *in vivo*, the body weights of mice were measured and mouse organs were collected, including the heart, liver, spleen and kidney, to observe changes in morphology by H&E staining. The mice appeared to tolerate erastin well, and neither a significant difference in body weight (Fig. 6J) nor noticeable organ damage (Fig. 6K) was detected between the treatment group and the control group.

Erastin synergistically enhances the growth inhibitory efficacy of docetaxel. Docetaxel, the standard therapy for CRPC, represents the only class of chemotherapy drugs that prolongs the survival of patients with CRPC. Previous studies have

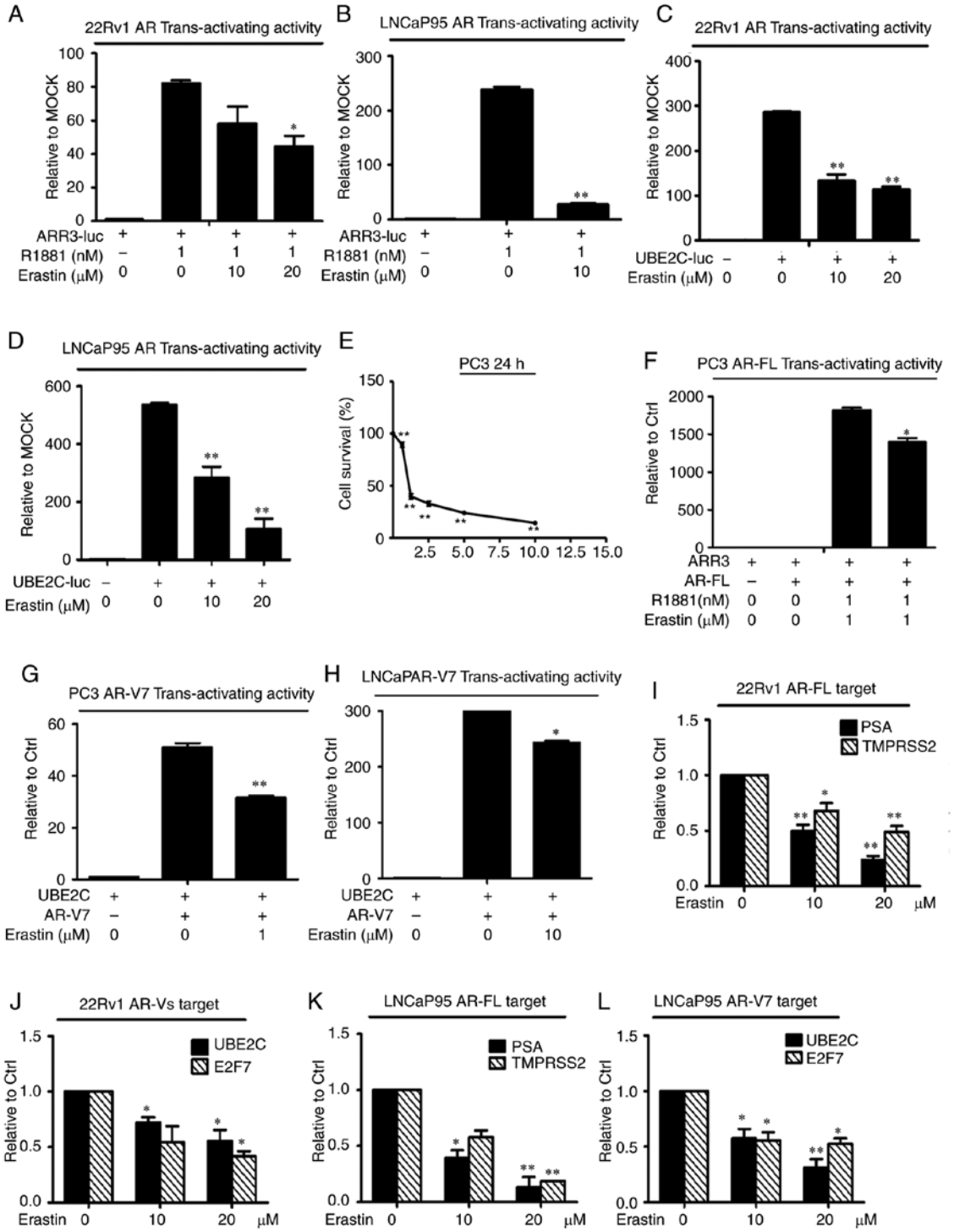

Figure 4. Erastin downregulates AR-FL and AR-V transactivation. A luciferase assay showed that erastin inhibited endogenous (A and B) AR-FL and (C and D) AR-V transcriptional activity. Cells transfected with the ARR3-luc or UBE2C-luc construct were treated with erastin. (E) Sulforhodamine B assays showed that erastin inhibited the growth of PC3 cells in a dose-dependent manner. Then, erastin inhibited exogenous (F) AR-FL and (G and H) AR-V transcriptional activity in PC3 and LNCaP cells. Reverse transcription-quantitative PCR analysis showed that erastin decreased the levels of (I and K) AR-FL target genes PSA and TMPRSS2 and (J and L) AR-V target genes UBE2C and E2F7. Statistical analysis was performed using ANOVA followed by Dunnett's post hoc test. $^{*}P<0.05$ and $^{**}P<0.01$ vs. control. AR, androgen receptor; AR-V, AR splice variant; AR-FL, AR full-length; PSA, prostate-specific antigen; TMPRSS2, transmembrane protease serine 2; UBE2C, ubiquitin-conjugating enzyme E2C; E2F7, transcription factor E2F7; luc, luciferase plasmid; ARR3, arrestin-C.

reported that docetaxel induces microtubule stabilization and abrogates AR nuclear translocation and transcriptional activity (29-31). However, microtubule stabilization has been found to have no effect on AR-Vs, especially AR-V7, with neither subcellular localization nor nuclear activity affected, indicating one of the mechanisms of docetaxel resistance (29,32). Given that erastin has the ability to downregulate AR-V expression and activity and that the underlying mechanism by which docetaxel inhibits AR-FL is different from that of erastin, it was hypothesized in the present study that

Table I. Combination index values of DTX and erastin treatment in 22Rv1 cells.

	Erastin, μM		
DTX, nM	2.5	5	10
5	0.313	0.717	0.989
10	0.550	0.615	0.252
20	0.480	0.706	0.821

Table II. Combination index values of DTX and erastin treatment in LNCaP95 cells.

	Erastin, μM		
DTX, nM	2.5	5	10
5	0.765	0.837	0.961
10	0.545	0.617	0.868

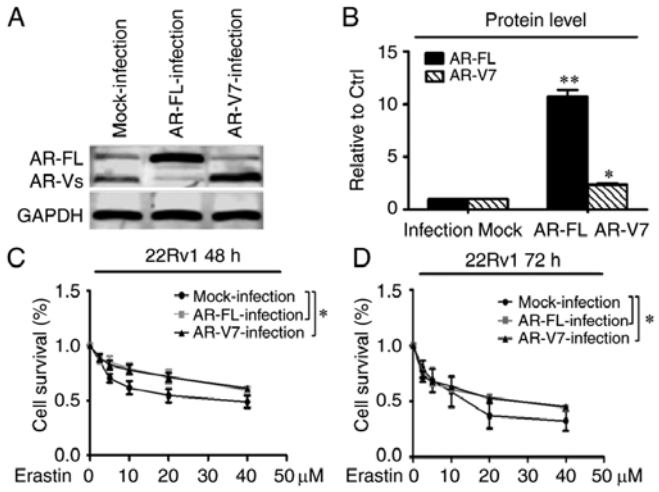

Figure 5. Attenuation of erastin growth inhibition by overexpression of AR-FL or AR-V7 in 22Rv1 cells. (A and B) 22Rv1 cells were infected with a construct expressing AR-FL or AR-V7, and western blotting revealed successful infection. assay was used to detect growth inhibition in cells (C) 48 and (D) 72 h after treatment with 0-40 μM erastin. Statistical analysis was performed using ANOVA followed by Dunnett's post hoc test. *P<0.05 and **P<0.01 vs. control. AR, androgen receptor; AR-V, AR splice variant; AR-FL, AR full-length.

erastin can enhance the efficacy of docetaxel in CRPC. To test this hypothesis, the growth of 22Rv1 and LNCaP95 cells was measured after treatment with erastin and docetaxel, and the combined index values were calculated. All the combinations produced a CI value <1, suggesting synergy between erastin and docetaxel in inhibiting cell growth (Tables I and II). When 5 μM erastin and 10 nM docetaxel were added to 22Rv1 and LNCaP95 cells alone or in combination, as shown in Fig. 7A and B, combination therapy inhibited tumor cell growth to a significantly greater extent than monotherapy. These data provided preliminary support for using erastin to enhance docetaxel efficacy in CRPC.

Discussion

As the first ferroptosis inducer discovered, erastin has been found to have a significant antitumor effect in multiple types of tumors through different mechanisms (33). However, there has been relatively little research on elastin in prostate cancer. In the present study, erastin inhibited the proliferation of 22RV1 and LNCaP95 cells in a dose-dependent manner. Although the mechanism of erastin-induced ferroptosis in prostate cancer remains unknown, the ferroptosis marker GPX4 protein was downregulated in both cell lines after treatment with erastin, indicating the inherent ferroptosis. In addition, it was confirmed that erastin can inhibit the expression of AR-FL and AR-V proteins by reducing the transcriptional activity of AR-FL and AR-Vs and downregulating the transcription level of the AR gene. In addition, *in vivo* experiments confirmed that erastin inhibited the growth rate of tumors and downregulated the levels of AR protein and mRNA in tumors. There was no evident damage induced by erastin, as the weight of the body and organs, such as the heart, liver, spleen and kidney, was unaffected in the treated in mice.

While, previous studies have confirmed that erastin exerts an antitumor effect in multiple types of cancer, such as colorectal, breast and cervical cancer (33-35), the results of the present study revealed a novel underlying mechanism in prostate cancer in which erastin reduces AR-FL and AR-V protein expression by downregulating their mRNA levels. The increased expression of the full-length and splice variants of AR has been indicated as an important mechanism of resistance to traditional androgen deprivation therapy and newly developed androgen deprivation drugs, such as abiraterone and enzalutamide (5,36,37). However, none of the anti-androgens currently used in clinics can target AR-Vs directly to reduce their availability. In addition to erastin, the selective AR degradants UT-69, UT-155 and (R)-UT-155 bind to the AR transcriptional activation domain AF-1 in the amino terminus, and UT-69 and UT-155 can also bind to the carboxy terminal LBD, significantly reducing the activity of wild-type and splice mutants even in the presence of small amounts of AR (38). ASC-J9, an AR degradation enhancer, can degrade both AR-FL and AR-V7 in 22Rv1 cells and in C4-2 and C81 cells upon the addition of AR-V7 (39). These compounds may serve as effective antidotes for overcoming resistance to androgen deprivation therapy for the treatment of CRPC in the future.

Erastin can also enhance the efficacy of docetaxel chemotherapy in prostate cancer (Fig. 7A and B). It is important for AR-FL to translocate from the cytoplasm to the nucleus to form dimers, which have transcriptional activity (29,30,40,41). Docetaxel has been reported to attenuate the nuclear input of AR-FL by stabilizing microtubules, which play important roles in the process of AR translocation (29). However, the nuclear localization of AR-Vs, especially AR-V7, is not dependent on microtubules, and AR-V expression is proposed to be one of the mechanisms of docetaxel resistance. The results of the present study showed that erastin enhanced the growth inhibitory effect of docetaxel in CRPC cells, thus it is necessary to

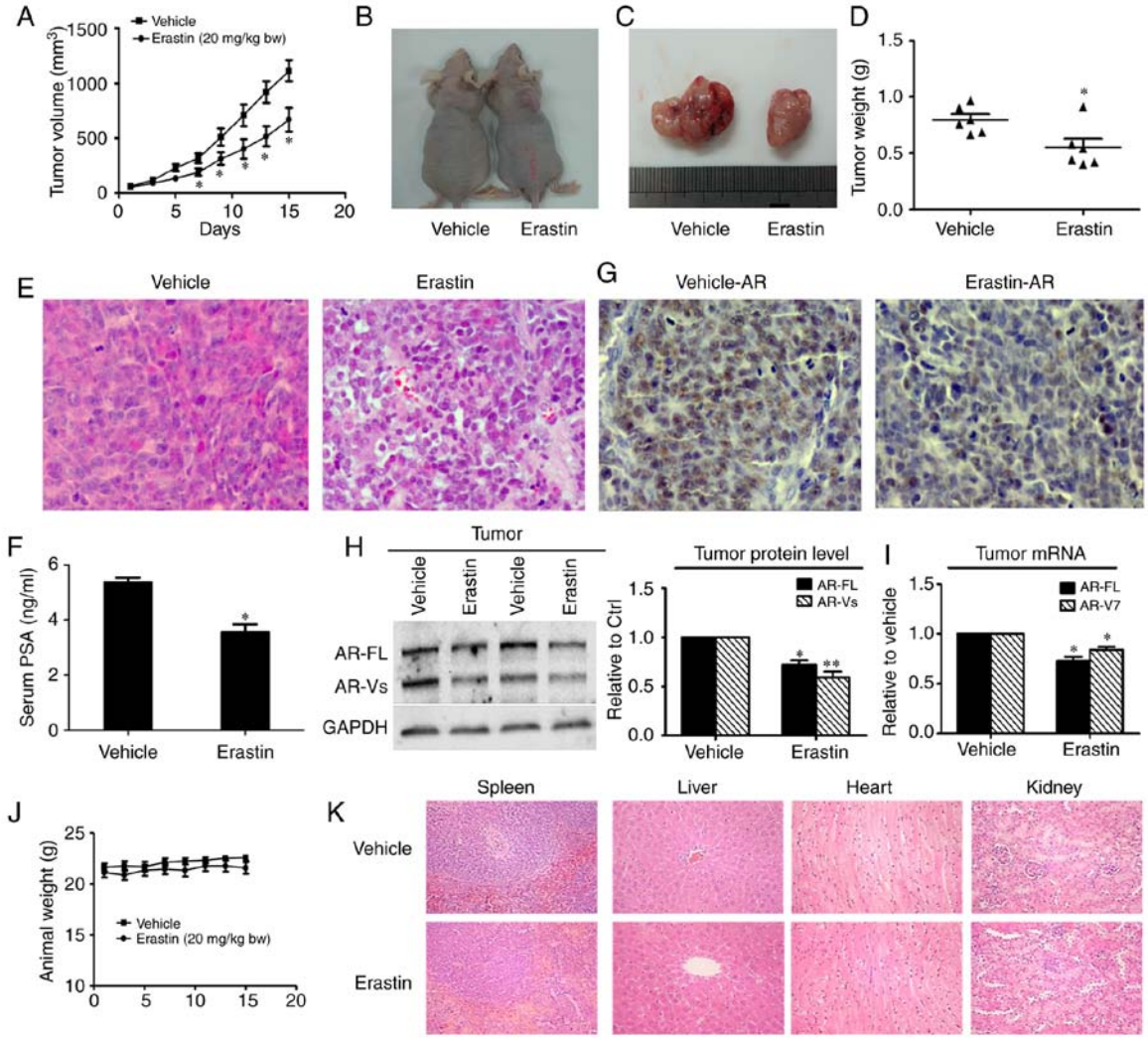

Figure 6. *In vivo* efficacy of erastin in the 22Rv1 xenograft model. (A) Mean tumor volumes (n=6). The (B) general condition of the mice and (C) representative tumor images. (D) Mean tumor weights. (E) Histopathological examination of 22Rv1 tumors by H&E staining (mmagnification, x200). (F) *In vivo* effect of erastin on serum PSA levels. (G) Representative immunohistochemistry images of AR in tumor tissues. (H) AR-FL and AR-V7 protein levels in the 22Rv1 xenograft model. (I) AR-FL and AR-V7 mRNA levels in the 22Rv1 xenograft model. (J) Mean body weights of the mice in each group. (K) H&E staining was used to evaluate the effect of erastin on the heart, liver, spleen and kidney of the mice (magnification, x200). Statistical analysis was performed using ANOVA followed by Dunnett's post hoc test. *P<0.05 and **P<0.01 vs. control. AR, androgen receptor; PSA, prostate-specific antigen; H&E, hematoxylin and eosin; AR-V, AR splice variant; AR-FL, AR full-length.

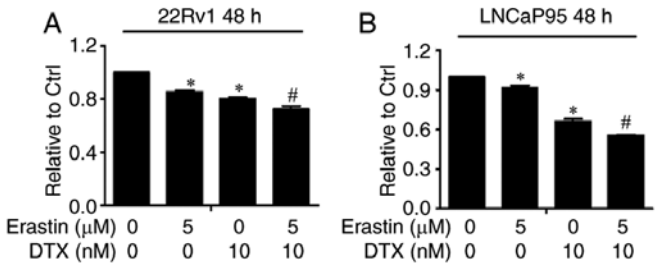

Figure 7. Erastin enhances docetaxel efficacy in prostate cancer cells. (A) 22Rv1 and (B) LNCaP95 cells were treated with 5 μM erastin with or without 10 nM DTX for 48 h, and cell growth was assessed using a sulforhodamine B assay. Statistical analysis was performed using ANOVA followed by Bonferroni's post hoc test. *P<0.05 vs. control; $^{\#}$P<0.05 vs. single-agent treatment groups. DTX, docetaxel.

determine the optimal ratio for the two drugs in combination therapy in future studies.

One of the chemotherapeutic mechanisms of docetaxel is the promotion of the mitochondrial release of cytochrome C, interrupting the mitochondrial electron transport chain, and leading to the production of a large amount of ROS, which cause lipid peroxidation, DNA oxidation modification, protein oxidation and inactivation of various enzymes, ultimately causing apoptosis and necrosis (42,43). However, when CRPC cells become resistant to docetaxel, the levels of ROS in cells are quite low (44,45). In the process of erastin-induced ferroptosis, the xCT light chain of the cystine/glutamate transporter is blocked, thus depleting GSH and reducing GPX4 activity, and as a result ROS cannot be catalyzed by GPX4. Ultimately, ROS accumulate, which can reverse the decrease in ROS levels caused by the docetaxel resistance of CRPC cells.

In summary, the present study demonstrated that erastin can significantly downregulate the expression and activities of AR-FL and AR-Vs in prostate cancer *in vitro* and *in vivo*, and enhance the growth inhibitory efficacy of docetaxel in CRPC

cells. These results indicated that erastin may be a promising therapeutic strategy for the treatment of human prostate cancer in the future, although further studies will be needed.

Acknowledgements

We would like to thank Dr Alan Meeker at the Johns Hopkins University (Baltimore, Maryland) for providing LNCaP95 cells, and to Dr Robert Matusik at Vanderbilt School of Medicine (Nashville, Tennessee) for providing the ARR3-luc construct.

Funding

This work was supported by the National Natural Science Foundation of China Project (grant nos. 81302206 and 81602228), Jilin Scientific and Technological Development Program (grant no. 20160101237JC), and Project of Jilin Provincial Department of Education (grant no. JJKH20170831KJ).

Availability of data and materials

The datasets used and/or analyzed during the current study are available from the corresponding author on reasonable request.

Authors' contributions

LZ, YY and TL designed and conducted the study. CH, HX, WeL, JC and SW performed the experiments. YY, TL and YJ performed the data analysis and interpretation. YX and WaL were responsible for data collection, validation and visualization. YY and TL drafted the manuscript with critical revision from LZ. LZ and YY confirm the authenticity of all the raw data. All authors read and approved the final manuscript.

Ethics approval and consent to participate

The present study was approved by the Animal Ethics Committee of Basic Medical College of Jilin University (approval no. 2016045).

Patient consent for publication

Not applicable.

Competing interests

The authors declare that they have no competing interests.

References

1. Bray F, Ferlay J, Soerjomataram I, Siegel RL, Torre LA and Jemal A: Global cancer statistics 2018: GLOBOCAN estimates of incidence and mortality worldwide for 36 cancers in 185 countries. CA Cancer J Clin 68: 394-424, 2018.
2. Ferraldeschi R, Welti J, Luo J, Attard G and de Bono JS: Targeting the androgen receptor pathway in castration-resistant prostate cancer: Progresses and prospects. Oncogene 34: 1745-1757, 2015.
3. Sun S, Sprenger CC, Vessella RL, Haugk K, Soriano K, Mostaghel EA, Page ST, Coleman IM, Nguyen HM, Sun H, *et al*: Castration resistance in human prostate cancer is conferred by a frequently occurring androgen receptor splice variant. J Clin Invest 120: 2715-2730, 2010.
4. Noble RL: The development of prostatic adenocarcinoma in Nb rats following prolonged sex hormone administration. Cancer Res 37: 1929-1933, 1977.
5. Egan A, Dong Y, Zhang H, Qi Y, Balk SP and Sartor O: Castration-resistant prostate cancer: Adaptive responses in the androgen axis. Cancer Treat Rev 40: 426-433, 2014.
6. Centenera MM, Harris JM, Tilley WD and Butler LM: The contribution of different androgen receptor domains to receptor dimerization and signaling. Mol Endocrinol 22: 2373-2382, 2008.
7. Chandrasekar T, Yang JC, Gao AC and Evans CP: Mechanisms of resistance in castration-resistant prostate cancer (CRPC). Transl Androl Urol 4: 365-380, 2015.
8. Hu R, Dunn TA, Wei S, Isharwal S, Veltri RW, Humphreys E, Han M, Partin AW, Vessella RL, Isaacs WB, *et al*: Ligand-independent androgen receptor variants derived from splicing of cryptic exons signify hormone-refractory prostate cancer. Cancer Res 69: 16-22, 2009.
9. Dolma S, Lessnick SL, Hahn WC and Stockwell BR: Identification of genotype-selective antitumor agents using synthetic lethal chemical screening in engineered human tumor cells. Cancer Cell 3: 285-296, 2003.
10. Dixon SJ, Lemberg KM, Lamprecht MR, Skouta R, Zaitsev EM, Gleason CE, Patel DN, Bauer AJ, Cantley AM, Yang WS, *et al*: Ferroptosis: An iron-dependent form of nonapoptotic cell death. Cell 149: 1060-1072, 2012.
11. Yagoda N, von Rechenberg M, Zaganjor E, Bauer AJ, Yang WS, Fridman DJ, Wolpaw AJ, Smukste I, Peltier JM, Boniface JJ, *et al*: RAS-RAF-MEK-dependent oxidative cell death involving voltage-dependent anion channels. Nature 447: 864-868, 2007.
12. Dixon SJ, Patel DN, Welsch M, Skouta R, Lee ED, Hayano M, Thomas AG, Gleason CE, Tatonetti NP, Slusher BS and Stockwell BR: Pharmacological inhibition of cystine-glutamate exchange induces endoplasmic reticulum stress and ferroptosis. Elife 3: e02523, 2014.
13. Sato M, Kusumi R, Hamashima S, Kobayashi S, Sasaki S, Komiyama Y, Izumikawa T, Conrad M, Bannai S and Sato H: The ferroptosis inducer erastin irreversibly inhibits system xc- and synergizes with cisplatin to increase cisplatin's cytotoxicity in cancer cells. Sci Rep 8: 968, 2018.
14. Yu Y, Xie Y, Cao L, Yang L, Yang M, Lotze MT, Zeh HJ, Kang R and Tang D: The ferroptosis inducer erastin enhances sensitivity of acute myeloid leukemia cells to chemotherapeutic agents. Mol Cell Oncol 2: e1054549, 2015.
15. Kwon MY, Park E, Lee SJ and Chung SW: Heme oxygenase-1 accelerates erastin-induced ferroptotic cell death. Oncotarget 6: 24393-24403, 2015.
16. Sun X, Ou Z, Chen R, Niu X, Chen D, Kang R and Tang D: Activation of the p62-Keap1-NRF2 pathway protects against ferroptosis in hepatocellular carcinoma cells. Hepatology 63: 173-184, 2016.
17. Hasegawa M, Takahashi H, Rajabi H, Alam M, Suzuki Y, Yin L, Tagde A, Maeda T, Hiraki M, Sukhatme VP and Kufe D: Functional interactions of the cystine/glutamate antiporter, CD44v and MUC1-C oncoprotein in triple-negative breast cancer cells. Oncotarget 7: 11756-11769, 2016.
18. Roh JL, Kim EH, Jang HJ, Park JY and Shin D: Induction of ferroptotic cell death for overcoming cisplatin resistance of head and neck cancer. Cancer Lett 381: 96-103, 2016.
19. Dong Y, Zhang H, Hawthorn L, Ganther HE and Ip C: Delineation of the molecular basis for selenium-induced growth arrest in human prostate cancer cells by oligonucleotide array. Cancer Res 63: 52-59, 2003.
20. Livak KJ and Schmittgen TD: Analysis of relative gene expression data using real-time quantitative PCR and the 2(-Delta Delta C(T)) method. Methods 25: 402-408, 2001.
21. Gordon CA, Gulzar ZG and Brooks JD: NUSAP1 expression is upregulated by loss of RB1 in prostate cancer cells. Prostate 75: 517-526, 2015.
22. Wu S, Zhao F, Zhao J, Li H, Chen J, Xia Y, Wang J, Zhao B, Zhao S and Li N: Dioscin improves postmenopausal osteoporosis through inducing bone formation and inhibiting apoptosis in ovariectomized rats. Biosci Trends 13: 394-401, 2019.
23. Zheng J, Zhao S, Yu X, Huang S and Liu HY: Simultaneous targeting of CD44 and EpCAM with a bispecific aptamer effectively inhibits intraperitoneal ovarian cancer growth. Theranostics 7: 1373-1388, 2017.
24. Dehm SM, Schmidt LJ, Heemers HV, Vessella RL and Tindall DJ: Splicing of a novel androgen receptor exon generates a constitutively active androgen receptor that mediates prostate cancer therapy resistance. Cancer Res 68: 5469-5477, 2008.

25. Kita K, Shiota M, Tanaka M, Otsuka A, Matsumoto M, Kato M, Tamada S, Iwao H, Miura K, Nakatani T and Tomita S: Heat shock protein 70 inhibitors suppress androgen receptor expression in LNCaP95 prostate cancer cells. Cancer Sci 108: 1820-1827, 2017.
26. Zhao N, Peacock SO, Lo CH, Heidman LM, Rice MA, Fahrenholtz CD, Greene AM, Magani F, Copello VA, Martinez MJ, *et al*: Arginine vasopressin receptor 1a is a therapeutic target for castration-resistant prostate cancer. Sci Transl Med 11: eaaw4636, 2019.
27. Xu D, Zhan Y, Qi Y, Cao B, Bai S, Xu W, Gambhir SS, Lee P, Sartor O, Flemington EK, *et al*: Androgen receptor splice variants dimerize to transactivate target genes. Cancer Res 75: 3663-3671, 2015.
28. Paschalis A, Sharp A, Welti JC, Neeb A, Raj GV, Luo J, Plymate SR and de Bono JS: Alternative splicing in prostate cancer. Nat Rev Clin Oncol 15: 663-675, 2018.
29. Thadani-Mulero M, Portella L, Sun S, Sung M, Matov A, Vessella RL, Corey E, Nanus DM, Plymate SR and Giannakakou P: Androgen receptor splice variants determine taxane sensitivity in prostate cancer. Cancer Res 74: 2270-2282, 2014.
30. Darshan MS, Loftus MS, Thadani-Mulero M, Levy BP, Escuin D, Zhou XK, Gjyrezi A, Chanel-Vos C, Shen R, Tagawa ST, *et al*: Taxane-induced blockade to nuclear accumulation of the androgen receptor predicts clinical responses in metastatic prostate cancer. Cancer Res 71: 6019-6029, 2011.
31. Zhu ML, Horbinski CM, Garzotto M, Qian DZ, Beer TM and Kyprianou N: Tubulin-targeting chemotherapy impairs androgen receptor activity in prostate cancer. Cancer Res 70: 7992-8002, 2010.
32. Bai S, Zhang BY and Dong Y: Impact of taxanes on androgen receptor signaling. Asian J Androl 21: 249-252, 2019.
33. Zhao Y, Li Y, Zhang R, Wang F, Wang T and Jiao Y: The role of erastin in ferroptosis and its prospects in cancer therapy. Onco Targets Ther 13: 5429-5441, 2020.
34. Huo H, Zhou Z, Qin J, Liu W, Wang B and Gu Y: Erastin disrupts mitochondrial permeability transition pore (mPTP) and induces apoptotic death of colorectal cancer cells. PLoS One 11: e0154605, 2016.
35. Yu M, Gai C, Li Z, Ding D, Zheng J, Zhang W, Lv S and Li W: Targeted exosome-encapsulated erastin induced ferroptosis in triple negative breast cancer cells. Cancer Sci 110: 3173-3182, 2019.
36. Antonarakis ES, Lu C, Wang H, Luber B, Nakazawa M, Roeser JC, Chen Y, Mohammad TA, Chen Y, Fedor HL, *et al*: AR-V7 and resistance to enzalutamide and abiraterone in prostate cancer. N Engl J Med 371: 1028-1038, 2014.
37. Li Y, Chan SC, Brand LJ, Hwang TH, Silverstein KA and Dehm SM: Androgen receptor splice variants mediate enzalutamide resistance in castration-resistant prostate cancer cell lines. Cancer Res 73: 483-489, 2013.
38. Ponnusamy S, Coss CC, Thiyagarajan T, Watts K, Hwang DJ, He Y, Selth LA, McEwan IJ, Duke CB, Pagadala J, *et al*: Novel selective agents for the degradation of androgen receptor variants to treat castration-resistant prostate cancer. Cancer Res 77: 6282-6298, 2017.
39. Yamashita S, Lai KP, Chuang KL, Xu D, Miyamoto H, Tochigi T, Pang ST, Li L, Arai Y, Kung HJ, *et al*: ASC-J9 suppresses castration-resistant prostate cancer growth through degradation of full-length and splice variant androgen receptors. Neoplasia 14: 74-83, 2012.
40. Zhang G, Liu X, Li J, Ledet E, Alvarez X, Qi Y, Fu X, Sartor O, Dong Y and Zhang H: Androgen receptor splice variants circumvent AR blockade by microtubule-targeting agents. Oncotarget 6: 23358-23371, 2015.
41. Shan X, Danet-Desnoyers G, Aird F, Kandela I, Tsui R, Perfito N and Iorns E: Replication study: Androgen receptor splice variants determine taxane sensitivity in prostate cancer. PeerJ 6: e4661, 2018.
42. Cristofani R, Montagnani Marelli M, Cicardi ME, Fontana F, Marzagalli M, Limonta P, Poletti A and Moretti RM: Dual role of autophagy on docetaxel-sensitivity in prostate cancer cells. Cell Death Dis 9: 889, 2018.
43. Wang L, Chen H, Liu F, Madigan MC, Power CA, Hao J, Patterson KI, Pourgholami MH, O'Brien PM, Perkins AC and Li Y: Monoclonal antibody targeting MUC1 and increasing sensitivity to docetaxel as a novel strategy in treating human epithelial ovarian cancer. Cancer Lett 300: 122-133, 2011.
44. Zhang D, Cui Y, Niu L, Xu X, Tian K, Young CYF, Lou H and Yuan H: Regulation of SOD2 and β-arrestin1 by interleukin-6 contributes to the increase of IGF-1R expression in docetaxel resistant prostate cancer cells. Eur J Cell Biol 93: 289-298, 2014.
45. Shan W, Zhong W, Zhao R and Oberley TD: Thioredoxin 1 as a subcellular biomarker of redox imbalance in human prostate cancer progression. Free Radic Biol Med 49: 2078-2087, 2010.